

Molecular Model for Toughening in Double-Network Hydrogels

Vijay R. Tirumala,[†] Taiki Tominaga,^{†,‡} Sanghun Lee,[†] Paul D. Butler,[§] Eric K. Lin,[†] Jian Ping Gong,[‡] and Wen-li Wu^{*,†}

Polymers Division and NIST Center for Neutron Research, National Institute of Standards and Technology, Gaithersburg, Maryland 20899, and Graduate School of Science, Hokkaido University, Sapporo, Japan 060-0810

Received: January 10, 2008; Revised Manuscript Received: April 4, 2008

A molecular mechanism is proposed for the toughness enhancement observed in double-network (DN) hydrogels prepared from poly(2-acrylamido-2-methyl-1-propanesulfonic acid) (PAMPS) polyelectrolyte network and poly(acrylamide) (PAAm) linear polymer. It is an extension of the phenomenological model set forth recently by Gong et al. (*Macromolecules* 2007, 40, 6658–6664). This mechanism rationalizes the changes in molecular structure of the DN gel constituents observed via in situ neutron scattering measurements, the composition dependence of the solution viscosity, and the thermodynamic interaction parameters of PAMPS and PAAm molecules obtained previously from neutron scattering studies. More specifically, this proposed mechanism provides an explanation for the observed periodic compositional fluctuations in the micrometer range induced by large strain deformation.

Introduction

The long-standing pursuit of a synthetic equivalent to soft tissues has recently seen significant activity with the development of new strategies for the synthesis of hydrogels. The class of materials termed nanocomposite (NC) hydrogels¹ and sliding (SR) gels² are both orders-of-magnitude more extensible than conventional hydrogels. In general, the individual network chains in permanently cross-linked hydrogels can be extended only within the mechanical constraints of cross-linked junction points. In both NC and SR gels, the junction points within the network are rendered mobile, which enables them to sustain high extensions by fully stretching the individual network chains.^{3–12} Whereas imparting extensibility to hydrogels might thus seem relatively straightforward, improving their compressive strength is not. Natural soft tissues such as articular cartilage contain >80% water by volume but can absorb as much as 700 J/m² under compression. Synthetic hydrogels, in contrast, become mechanically weak to sustain large compressions when the composition of water is increased beyond 70% by volume. In this context, the recently discovered double-network hydrogels (>85% water by volume) and the molecular origin responsible for their superior compressive strength (~400 J/m²) assume greater significance in our quest to develop synthetic mimics for naturally occurring soft materials.^{13–17}

Double-network hydrogels (DN gels) are prepared by simply incorporating a solution of high-molar-mass linear polymer within a moderately cross-linked but fully swollen charged polymer network.¹³ A number of different polymer pairs have been used to prepare DN gels, and their compressive strengths have been found, in general, to be greater than those of the individual components. In a fully swollen state, the permanently cross-linked charged polymer (polyelectrolyte) network is mechanically rigid but too brittle to sustain compression. The

high-molar-mass linear polymer solution, in contrast, is extremely soft and readily deformable. Because neither of the components is individually tough enough to resist deformation, the synergistic mechanism responsible for the superior compressive strength or fracture toughness of DN gels is intriguing and has attracted significant recent attention.^{18–20}

A mechanism to account for the superior toughness of DN gels was first proposed by Gong et al.^{21,22} They proposed that a multiple fracture process that turns the polyelectrolyte network into pieces of a few hundred nanometers in the linear dimension provides a pathway for irreversible energy dissipation. This mechanism was further supported by two recent studies based on detailed mechanical measurements.^{23,24} It is plausible that a multiple fracture of the polyelectrolyte network with the fracture surfaces bridged and stabilized by linear chains would lead to an enhancement in fracture strain and other related mechanical properties. However, the molecular attributes that will allow for multiple fracture of the first network, which is central to the deformation process proposed by Gong et al., have not yet been discussed. The stabilization mechanism through which the initial cracks in the polyelectrolyte network are hindered from coalescing to result in catastrophic sample failure is also unclear. The purpose of this work is to develop a molecular model to detail some of the necessary and sufficient conditions for multiple fractures to occur in the polyelectrolyte network of DN gels.

Throughout this work, the polyelectrolyte is designated as component 1, the linear chains as component 2, and the solvent as component 3. As suggested in Gong et al.'s model, the linear polymer chains bridging the cracks can stabilize them similarly to the role played by craze in glassy polymers. The simplest model to describe the mechanical behavior of linear chains bridging the cracks follows rubber elasticity; that is, the force to stretch these linear chains increases with strain until the local stress equals the applied stress. The underlying premise for the abovementioned chain stretching process to work is that the linear chains are anchored within the network or component 1 instead of endlessly sliding out of the network. Strain hardening

* Corresponding author. E-mail: wenli@nist.gov.

[†] Polymers Division, National Institute of Standards and Technology.

[‡] Hokkaido University.

[§] NIST Center for Neutron Research, National Institute of Standards and Technology.

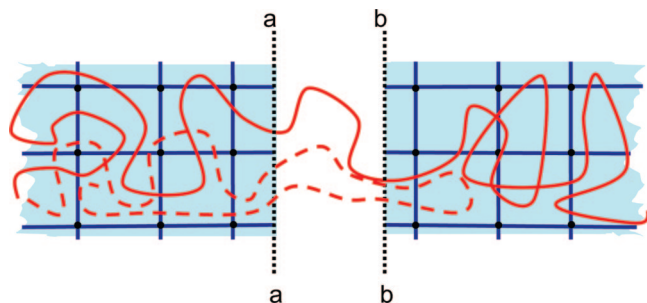


Figure 1. Schematic of a crack inside DN gel. The fracture surfaces *a*–*a* and *b*–*b* of the PAMPS network are bridged by PAAm chains depicted as red lines. The solid red line denotes a tie chain along which the local stress can be transferred effectively, whereas the dashed line denotes a chain that is shallowly buried on one side of a crack and hence is not an effective stress-bearing chain across the crack.

during the reloading cycle of the hysteresis stress loop in deformed DN gel has been reported and modeled with rubber elasticity theory.²⁴ The specific DN gels in that study were prepared from the combination of poly(2-acrylamido-2-methyl-1-propanesulfonic acid) (PAMPS; component 1) and poly(acrylamide) (PAAm; component 2). This observation provides the stabilization mechanism for the exposed PAAm chains bridging the cracks provided that they are anchored inside the PAMPS network. Both covalent bonding and topological entanglement between components 1 and 2 can address this anchoring requirement. However, the analysis of small-angle neutron scattering from PAMPS/PAAm DN gels and their solution mixture analogs has shown that chemical association between components 1 (polyelectrolyte) and 2 (neutral polymer) is predominant in DN gels, $\chi_{12} \ll \chi_{1s} < \chi_{2s}$ ($0.05 \ll 0.32 < 0.45$).²⁵ Therefore, we propose a new deformation mechanism that considers association between the components.

An effective stress-transfer mechanism between the bridging linear chains and the network chains on which they are anchored is a necessary condition for additional cracks to develop near an existing crack and is illustrated in Figure 1. From a simple force balance consideration, the PAAm chains bridging the crack between surfaces *a*–*a* and *b*–*b* must carry a load equal to the applied stress. At a certain distance from the initial crack, the majority of the applied stress must be carried by the rigid PAMPS network. The distance at which stress is effectively transferred is the cornerstone of the deformation mechanism to be discussed. We address how the force exerted on the PAAm chains is transferred to the network chains or the PAMPS molecules. The extent of force transfer must be sufficient to cause the PAMPS network to crack at a distance l_c from the initial crack. Following the spirit of the model developed many decades ago²⁶ for fiber-reinforced composites, we propose a similar shear-lag model. In this model, the applied stress is transferred from the PAAm chains to the PAMPS network gradually via adhesion force (a shear stress) between these two components. The major difference between the fiber pullout process and the present model is the site of fracture. In fiber pullout, the reinforcing fiber breaks into multiple segments, and the applied tensile load is transferred from the soft matrix to the fiber through the fiber/matrix interface. In the present case, the PAAm chains play the role of a flexible embedding matrix, whereas the PAMPS network plays the role of rigid fiber in which fracture takes place. However, the load transfer still relies on adhesion between the reinforcing fiber and the matrix, which, in the present case, corresponds to the adhesion or association between the PAMPS and PAAm molecules.

The rest of this article is divided into four sections: (i) a summary of the experimental findings from neutron scattering data on DN gels subjected to pure shear deformation; (ii) a semiquantitative calculation of the minimum size, l_c , of the PAMPS network capable of anchoring the PAAm chains; (iii) a revisiting of Figure 1 to discuss an important shortfall implicated in this highly simplified one-dimensional deformation model; and (iv) conclusions.

Materials and Methods

Materials Used. 2-Acrylamido-2-methyl-1-propanesulfonic acid (AMPS) (monomer; TCI America) and 2-oxoglutaric acid (initiator; Polysciences, Inc.) were used as received. Acrylamide monomer was recrystallized from chloroform. Deuterated acrylamide monomer (d_3 -AAM; Cambridge Isotope Laboratories, Inc.) free of inhibitor was used as received. *N,N'*-Methylene bisacrylamide (cross-linker) was recrystallized from ethanol.²⁷ Deuterated water was used as received from Aldrich.

Sample Preparation. DN gels were prepared from a combination of an anionic polyelectrolyte and a neutral polymer following the previously established procedure.¹³ PAMPS/PAAm DN gel samples were prepared by polymerizing acrylamide monomer within the PAMPS network swollen in water at a 1:20 PAMPS/AAM molar ratio. Samples were prepared in triplicate with the same PAMPS/AAM composition but at different neutron scattering contrast conditions to independently ascertain the component morphologies. The in situ morphology of PAAm linear chains and the morphologies of the PAMPS network the total DN gel were determined by (i) polymerizing deuterium-labeled acrylamide monomer (d_3 -AAM) within a PAMPS network swollen in water, (ii) polymerizing d_3 -AAM in a PAMPS network swollen in a mixture of light and heavy water at appropriate hydrogen/deuterium ratios (71:29) to achieve contrast matching conditions for d_3 -AAM, and (iii) preparing PAMPS/PAAm DN gels in heavy water, respectively.²⁸ The volumetric swelling degree of the primary PAMPS network used in all samples was about 50, which corresponds to a nominal polymer concentration of 0.1 mol/L in the fully swollen state. The cross-link density corresponding to the swelling degree was estimated from Flory–Rehner theory to be 1.9×10^{-5} mol/cm³.²⁹

In Situ Deformation of DN Gels for SANS. A sample cell was specifically designed to study the morphology of DN gels subjected to pure shear deformation.²⁸ Within this cell, the specimen was elongated along the *y* axis by compression along the *z* axis while maintaining a constant width (*x* axis). This design minimizes the potential for the formation of cracks or microvoids, features that would also scatter neutrons, because no tensile stress is exerted on the specimen. The incident neutron beam was along the normal (*z* axis) of the sample surface designated as the *x*–*y* plane.

Neutron Scattering. Neutron scattering measurements were conducted at the National Institute of Standards and Technology Center for Neutron Research (NCNR) using three spectrometers (NG3, NG7, and BT5) to probe structural information in a reciprocal scattering vector space, $q = 2\pi/\xi$, where ξ is the real-space correlation length ranging from nanometers to micrometers.^{30,31} Both NG3 and NG7 are instruments with pinhole collimation and a 2D detector with a q range from 2×10^{-3} to 0.18 \AA^{-1} . BT5 is a Bonse–Hart instrument capable of covering a q range from 5×10^{-5} to 10^{-3} \AA^{-1} .

SANS Data Processing. SANS and ultra-SANS (USANS) data were reduced into absolute intensity units by subtracting contributions from the instrument background, scattering from

quartz windows of empty compression cell, and incoherent scattering from the sample and correcting for variations in the detector sensitivity following established procedures.³² Scattering intensity in absolute units was then normalized by the neutron contrast factor, $(b_1 - b_s)^2$, and the volume fraction factor, $\varphi_i(1 - \varphi_i)$, as described previously.²⁸ This normalization facilitates direct comparison of the results by removing variations in neutron scattering intensity due to changes in the neutron contrast and/or polymer composition.

Rheological Measurements. Rheological measurements on the solution blend analogs of PAMPS/PAAm DN gels were performed using an Advanced Rheometric Expansion System (ARES-LS, TA Instruments). Viscosity measurements were performed in a steady-shear sweep mode, and the data points at a certain shear rate were obtained as an average over 1 min. Aqueous solutions of PAMPS and PAAm were prepared separately by photopolymerization at a concentration of 0.2 mol/L. The concentrations of photoinitiator were 0.1 and 1 mol % relative to the AAm and AMPS monomers, respectively. Molecular parameters such as molar mass and molar mass distribution were measured from samples diluted by an aqueous solution of sodium nitrate using gel permeation chromatography. The strongly charged PAMPS homopolymer solution was neutralized before the measurement using sodium hydroxide. PAAm had a number-average molar mass of approximately 6×10^5 g/mol and a polydispersity index of 2, and the corresponding values for PAMPS were 1.9×10^5 g/mol and 1.45, respectively. Blend samples were prepared by mixing the polyelectrolyte and neutral polymer solutions at a given volume ratio. Note that a 1:20 molar ratio corresponds to a 1:7 volume ratio for PAMPS/PAAm, as discussed previously.²⁸

Neutron Scattering Results

SANS measurements on all the samples were performed to characterize the structure of each polymer component as well as the total polymer structure within the PAMPS/PAAm DN gel before, during, and after pure shear deformation. The imposed strain was maintained at a constant value of 50% in compression along the z axis in all measurements, which translates into an extensional strain of 100% along the y axis. Some of the SANS data end in the vicinity of $5 \times 10^{-4} \text{ \AA}^{-1}$ instead of at the lowest accessible q value (10^{-5} \AA^{-1}). For example, in Figure 2, the data from the deformed sample along the stretch direction cover the low- q region, whereas the rest end abruptly at higher q . This is because the BT5 instrument, a Bonse–Hart diffractometer used for the ultralow- q measurements, has significant background noise; the level of this noise increases as q approaches zero. Data from samples with scattering intensities near the background noise level were simply discarded.

The neutron scattering intensity from samples in the deformed state was anisotropic in the USANS region. Hence, the sector averages of the scattering intensity both parallel and perpendicular to the deformation axis are presented. SANS data from samples after the deformation had relaxed were also collected and are presented in this work because the information from relaxed samples provides some clue about the reversibility of the molecular displacement caused by deformation. The scattering intensity from samples before and after deformation was isotropic, and the data were azimuthally averaged.

Figure 2 shows that the scattering intensity³³ from linear PAAm chains (contrast condition i) is enhanced upon deformation, both parallel and perpendicular to the stretch direction. Along the extension axis, deformation gives rise to not only an

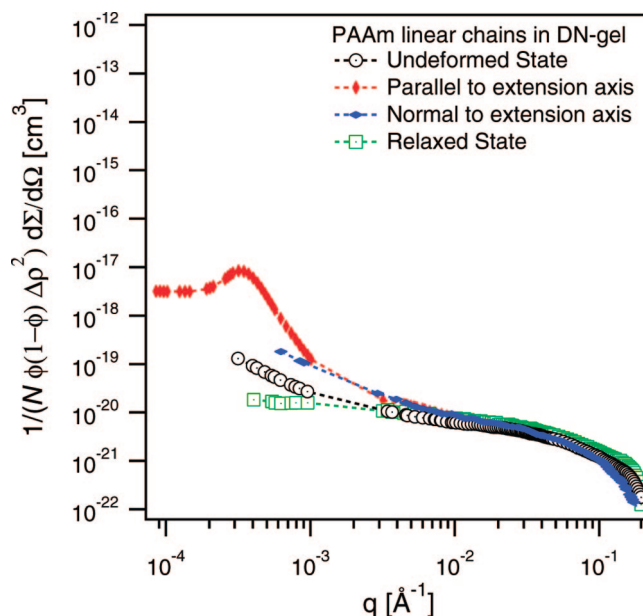


Figure 2. Neutron scattering from PAAm measured in situ for deformed DN gels (contrast condition i). Data parallel and normal to the elongation direction (y axis) are shown in red and blue, respectively. Results from the sample both before deformation (black) and after the deformation is relaxed (green) are also included for comparison. Markers are experimental data points, and dashed lines are drawn as a guide to the eye.

increase in scattering intensity but also a prominent maximum at $4.2 \times 10^{-4} \text{ \AA}^{-1}$. This represents a deformation-induced concentration fluctuation of PAAm chains at a length scale of around 1.5 \mu m . Such a large-scale and periodic concentration fluctuation is not predicted by any existing deformation models for DN gels; it is the cornerstone for the deformation mechanism proposed in this work. The importance of this observation is not just the observed length scale of 1.5 \mu m but also the periodic nature of concentration fluctuations. This indicates that the periodic concentration fluctuations occur throughout the entire sample volume instead of being localized near cracks as in the case of brittle materials. After the deformation is removed and the sample is restored to its original macroscopic dimensions, the SANS data indicate that the periodicity of concentration fluctuations disappears completely. The data in Figure 2 actually show a decrease in scattering intensity from the sample after the deformation is removed. The significance of this observation is currently unclear.

The SANS results presented in Figure 3 indicate that deformation also induces an increase in scattering intensity from the PAMPS network (contrast condition ii) both parallel and perpendicular to the stretch direction. In contrast to the results for the PAAm chains, the increase in scattering intensity from the PAMPS network is larger in the direction perpendicular to extension than in the parallel direction. Also, for both PAMPS and PAAm, the difference in scattering intensity between parallel and perpendicular directions is close to 2 orders of magnitude in the low- q region. The deformation-induced increase in scattering intensity parallel to the extension axis is thus nearly 1000 times higher than that from the sample in the undeformed or relaxed state, which is well above the $\pm 10\%$ uncertainty in the intensity measurement. There also exists a rather weak intensity maximum in scattering parallel to the extension axis at the same q position as for the PAAm case. However, restoring the sample to its original macroscopic size does not result in a complete recovery of the intensity from the PAMPS network

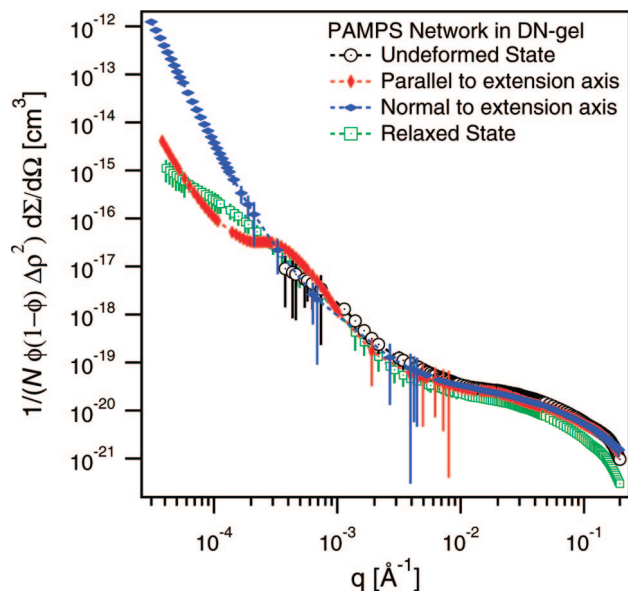


Figure 3. Neutron scattering from PAMPS network of DN gel measured in situ for deformed DN gels (contrast condition ii). Data parallel and normal to the elongation direction (y axis) are shown in red and blue, respectively. Data from the sample both before deformation (black) and after the deformation is relaxed (green) are also included for comparison. In the ultralow- q region from 5×10^{-4} to $5 \times 10^{-5} \text{ \AA}^{-1}$, the scattering intensity of the sample before deformation is barely above the background level of the Bonse–Hart diffractometer and hence is not shown.

to that in the undeformed state. The scattering pattern recorded on the 2D detector became almost isotropic, and the intensities stayed at an elevated level. This is in contrast to the results for PAAM. This observation provides unambiguous evidence for permanent changes in network structure due to deformation, most likely the formation of multiple cracks in the PAMPS network.

The SANS results for the total polymer structure, that is, a combination of both PAMPS and PAAM molecules appear to be one species under neutron contrast condition iii, are shown in Figure 4. Because PAAM is the major component of the polymer with a 7:1 PAAM/PAMPS volume ratio, it is rather surprising to find that the deformation-induced changes in the total polymer structure do not follow those of PAAM. Enhancement in scattering intensity was observed along the direction parallel to extension, but the scattering maximum near $4.2 \times 10^{-4} \text{ \AA}^{-1}$ almost disappeared. This is indicative of the complementary or out-of-phase nature of the concentration fluctuations of PAMPS and PAAM; that is, within the deformed DN gels, the high-concentration region of PAAM is located in the low-concentration region of PAMPS and vice versa. In other words, the deformation-induced compositional fluctuations in PAMPS and PAAM are out-of-phase. Otherwise, one would expect a prominent scattering maximum to also appear in the total network structure factor.

The periodicity of concentration fluctuations observed from DN gels under pure shear deformation is rather large at $\sim 1.5 \text{ \mu m}$ and has not been previously reported in experiments on similar systems. Cross-linked polymer networks and hydrogels, for example, display so-called butterfly or inverse-butterfly patterns when subjected to uniaxial extension.^{34–37} The observed scattering intensity in such patterns, however, is strongly anisotropic at small length scales and decays monotonically with q but does not result in a prominent scattering maximum when the data are azimuthally averaged. Therefore, the proposed

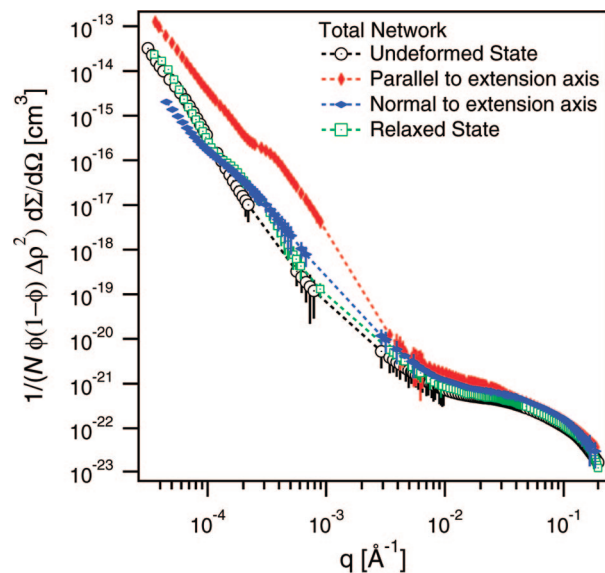


Figure 4. Neutron scattering from the total network measured in situ for deformed DN gels (contrast condition iii). Data parallel and normal to the elongation direction (y axis) are shown in red and blue, respectively. Results from the sample both before deformation (black) and after the deformation is relaxed (green) are also included for comparison. Markers are experimental data points, and dashed lines are drawn as a guide to the eye.

deformation model should account for the formation of multiple cracks with a modestly regular intercrack spacing within the PAMPS network.

Molecular Model for Deformation of DN Gels

Stress-Transfer Mechanism. We next propose a mechanism for stress transfer from the PAAM chains bridging the existing cracks to the PAMPS network next to the crack. This mechanism is built by following the spirit behind the single-fiber fragmentation (SFF) measurement used in fiber-reinforced composites to evaluate the interfacial strength between fiber and matrix.^{26,38} In fiber-reinforced composites, the fiber typically has a higher modulus and a lower fracture strain than the matrix. The test sample in SFF measurements consists of one fiber with a sufficient aspect ratio embedded in a matrix, and the sample cross section is greater than that of the fiber by several orders of magnitude. The tensile load is applied on the matrix and is transmitted to the fiber through the fiber/matrix interface characterized by the magnitude of interfacial shear strength, τ_c . When sufficient tensile force is applied, multiple cracks occur along the fiber until its length between cracks reaches a critical length, l_c , below which load cannot be adequately transmitted from the matrix to the fiber through the interface. This fiber fragmentation length, l_c , is related to the mechanical properties of the constituents by the expression

$$l_c = \frac{3\sigma_f d_f}{8\tau_c} \quad (1)$$

where σ_f and d_f are the tensile strength and the diameter of the fiber, respectively. The factor 3/8 is included in the above equation to account for the statistical distribution of fiber segment lengths. Simple mechanical reasoning would otherwise lead to a factor of 1/2. For the present case of DN gels, the external load is exerted on the PAAM chains within a crack and is transmitted to the brittle PAMPS network next to the crack to induce additional cracks to occur. In this instance, the

PAAM chains play the role of the matrix, and the PAMPS network acts as the fiber. Aside from this obvious difference in sample geometry between SFF samples and DN gels, there are other differences worth mentioning. For example, the PAAM chains are not aligned with respect to the applied load direction, and numerous PAAM chains bridge a crack rather than a single chain. For simplicity, we use a mean-field approach to set up the fracture criterion in the DN gels as follows: The load carried by a PAAM chain needs to reach a value of $A\sigma_{1c}$ instead of $(\pi d_l^2 \sigma_l)/4$, where A represents the average area occupied by a single PAAM chain on a fracture surface and σ_{1c} is the fracture stress of the PAMPS/PAAM gel away from the initial crack. The value of σ_{1c} is set to be 0.2 MPa based on previous work.³⁹ Accordingly, eq 1 for the present case can be modified as

$$L_c = \frac{\sigma_{1c} A}{\pi \tau_c d_2} \quad (1')$$

where L_c denotes the contour length of the PAAM chain under tensile stress and the corresponding distance projected along the applied tensile stress direction is denoted as t_c . Thus, t_c is the minimum PAMPS fragment size that exists within a deformed DN gel along the tensile direction. The diameter, d_2 , of PAAM chain in eq 1' is approximated by $V_2^{1/3}$, where V_2 is the molar volume of a PAAM repeat unit of 82.54 Å³/mol; hence, $d_2 = 4.35$ Å. The local stress will not reach a value of σ_{1c} to cause additional fracturing if the size of PAMPS fragment is below $2t_c$. The experimentally observed repeat distance will be the sum of $2t_c$ and the crack width bridged by PAAM chains. A factor of 2 is included because the local tensile stress in a fragmented DN gel block has to reach σ_{1c} from both ends of the block. It is noteworthy that the value of t_c depends only on the properties of the constituents and the composition, but not on the applied stress.

The average area of the fracture surface per load-bearing PAAM chain across the crack shown in Figure 1 is denoted by A . Its value cannot be simply defined because a certain fraction of the chains bridging the crack are not load-bearing if their anchoring depths inside the PAMPS network are far less than t_c . For example, the chain represented by the dashed line in Figure 1 may not be a load-bearing chain because of its shallow anchoring depth within the PAMPS network on the right-hand side. As a first order of approximation, we propose that $A = cd_2^2/\phi_2$, where ϕ_2 denotes the volume fraction of the PAAM component and the factor c is introduced to account for the fact that only a fraction of the chains bridging a crack can be considered as load-bearing or tie chains. Based on our knowledge of oriented semicrystalline polymers, we estimated the magnitude of c to be on the order of 10^1 – 10^2 ; that is, only a few percent of the chains between crystallites can be considered as load-bearing chains.⁴⁰

To relate L_c to t_c , we simply take $t_c = (L_c/3l)^{0.5}b$, where b denotes the repeat length of a PAAM chain. Its value was taken to be 4.5 Å by accepting a characteristic ratio of 8.5 between the unperturbed dimension, h_0^2 , of PAAM in water and nl^2 , where n is the number of repeat units and l is the repeat distance of 1.54 Å.⁴¹ The factor of 3 in the denominator reflects the condition that only one-third of the repeat units, on average, are perpendicular to the crack.

If all of the above considerations are combined, the critical length t_c along the tensile direction can be expressed as

$$t_c = \left(\frac{cd_2\sigma_{1c}}{3\pi\phi_2\tau_c l} \right)^{0.5} b \quad (2)$$

Estimation of Interfacial Shear Strength, τ_c . The remaining question is to estimate the value of τ_c , the critical shear stress required to detach a PAAM segment from the PAMPS network. The energy, E_s , required to separate a PAAM/PAMPS contact is related to the quantity $(\chi_{1s} + \chi_{2s} - \chi_{12})$, as the separated PAMPS and PAAM segments are now in contact with water. More explicitly, one expects that

$$E_s \propto \phi_1(\chi_{12} - \chi_{1s} - \chi_{2s}) \frac{RT}{4N_A V_s} \quad (3)$$

where R is the gas constant, T is the temperature in Kelvin, N_A is Avogadro's number, and V_s is the molar volume of water (29.85 Å³/mol). The term ϕ_1 is included in the above equation to account for the conditional probability for the presence of a PAMPS segment in contact with the PAAM segment under consideration. For the samples studied in this work, the value of ϕ_1 was determined from swelling degree measurements to be 0.012. Estimating the magnitude of the critical shear stress, τ_c , for detaching a PAAM chain in contact with PAMPS from the value of E_s is not straightforward, given that it depends on the details of the deformation process at the atomistic scale. For example, one cannot possibly estimate the yield stress of a metal from its heat of evaporation. Nonetheless, one expects that the value of τ_c will scale with the magnitude of $(\chi_{1s} + \chi_{2s} - \chi_{12})$. In PAMPS/PAAM DN gels, the values of both χ_{1s} and χ_{2s} are rather high, whereas the value of χ_{12} is small, which suggests that strong binding exists between these two polymers when dissolved in water.

To estimate the value of τ_c , we used viscosity measurement results to determine the value of the monomer friction coefficient, ζ , in PAMPS/PAAM solution blends with molar ratios close to that of the DN gels studied herein. As reported in our previous work,²⁸ the zero-shear viscosity, η_0 , of the solution blends reaches a maximum at a 7:1 volumetric ratio of PAAM to PAMPS. The value of η_0 is 4×10^{-3} , 4×10^{-4} , and 1.6×10^{-5} N·S/cm² for PAAM concentrations (volume fractions, ϕ_2) of 0.022, 0.0088, and 0.044, respectively. Based on the work by van Meerveld,⁴² the following relation between η_0 and ζ was derived

$$\frac{\eta_0}{\zeta} = \frac{0.051(\rho N_A)^{3/4}}{3\pi^2 M_0^{4/3} M_e^{2.4}} M^{3.4} \phi_2^{3.4} \quad (4)$$

where ρ denotes the PAAM density, M_0 the monomer molecular weight, and M_e the entanglement molecular weight of PAAM in the bulk. The value of M_e was chosen to be 10⁴ g/mol following Kulicke et al.⁴³ In deriving the above equation, we invoked the relation that the entanglement molecular weight in solution scales as $1/\phi_2$.⁴⁴ The molecular weight of the PAAM used in the solution viscosity work was on the order of 10⁶ g/mol, and from the above-mentioned viscosity data, the calculated monomer friction coefficient, ζ , was determined to be 6.9×10^{-6} – 11 N·S/cm, a value close to that of bulk polystyrene at 100 °C above its glass transition temperature (Table 12-III, ref 43). In the above calculation, the combination of PAMPS chain and water was treated as the solvent. The zero-shear viscosity of PAAM solution is lowered by an order of magnitude in the absence of PAMPS. We assume that the monomer friction coefficient is reduced by a similar factor.

Estimation of Crack Periodicity. This value of 6.9×10^{-6} – 11 N·S/cm for the monomer friction coefficient was used to

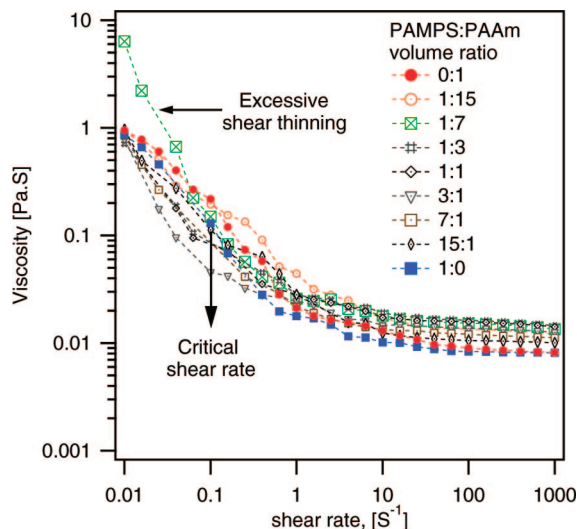


Figure 5. Viscosity of PAMPS/PAAM solution blends measured as a function of shear rate for various PAMPS/PAAM volume ratios. Each blend sample was prepared by mixing stock PAMPS and PAAM solutions of 0.2 mol/L concentration. An enhancement in viscosity at low shear rate is observed for 1:7 PAMPS/PAAM blend, but the viscosity rapidly decreases to a value similar to that of pure PAMPS solution beyond a critical shear rate of 10^{-1} S^{-1} as marked by the arrow.

estimate the value of τ_c appearing in eq 2 and, hence, the value of t_c for DN gels. This is reasonable given that the PAMPS/PAAM composition of the DN gel studied in this work was close to that of the measured solution. The value of τ_c can be replaced by $\zeta v l d_2^2$, where v is the maximum velocity above which the PAAM chain will be detached from PAMPS/PAAM association. Its value is approximated as $d_2 \dot{\gamma}$, where $\dot{\gamma}$ is the maximum shear rate above which the PAMPS/PAAM association becomes unstable. As discussed earlier, d_2 is the diameter of the PAAM chain and is equal to 4.35 Å. Equation 2 can now be expressed as

$$t_c = \left(\frac{c}{\dot{\gamma}}\right)^{0.5} \left(\frac{d_2^2 \sigma_{1c}}{3\pi\phi_2 \zeta l}\right)^{0.5} b \quad (2')$$

With $\sigma_{1c} = 0.2 \text{ MPa}$,³⁹ $\phi_2 = 0.09$, $d_2 = 4.35 \text{ Å}$, $l = 1.54 \text{ Å}$ and $b = 4.5 \text{ Å}$, the above equation can be reduced to

$$t_c = 0.092 \left(\frac{c}{\dot{\gamma}}\right)^{0.5} \mu\text{m S}^{-0.5} \quad (2'')$$

Recall that the parameter c is equal to the inverse of the fraction of load-bearing chains across a crack; for example, the value of c is 10 when 10% of the PAAM chains across a crack are load-bearing. $\dot{\gamma}$ is the critical shear rate in units of S^{-1} and can be estimated from the rheological behavior of the PAMPS/PAAM solution blend as follows: We noticed that the solution blend with enhanced viscosity also exhibited an excessive shear thinning as shown in Figure 5. Above a shear rate near 0.1 S^{-1} , the enhanced viscosity approached that of the pure PAMPS solution; hence, this shear rate was taken as the critical shear rate, $\dot{\gamma}$, above which the PAMPS/PAAM association becomes unstable. Using this value in eq 2'', we obtain a value of $0.29 \mu\text{m}$ for t_c even when c is taken at its minimum value of unity; that is, every single PAAM chain at the crack surface is load-bearing. As discussed previously, the average repeat distance in a deformed sample is the sum of $2t_c$ and the gap between the opposite surfaces of a crack. If the elastic strain of the fragmented PAMPS network blocks is neglected, the gap width

is simply the product of total extensional strain ($\epsilon \approx \Delta L/L$) along the tensile axis and the block length, which is just $2t_c$. The total periodicity thus becomes $2t_c(1 + \epsilon)$. This estimate yields a repeat distance of $1.16 \mu\text{m}$, as the tensile strain in the deformation SANS measurements is about 100%. This value is of the same order of magnitude as the experimentally observed value of $1.5 \mu\text{m}$ for the repeat distance.

Discussion

The relation $t_c \propto (L_c/3l)^{0.5}$ merits further consideration. In the spirit of the reptation model for polymer melts, one often takes L_c as the contour length of the chain. For the present case of DN gels, however, the total polymer concentration is only about 10 vol %, and under tensile stress, the PAAM chains will not be pulled out along their original contour length or within a tube. Many slacks, kinks, and bends along a PAAM chain surrounded by water will surely be pulled out, and the chain will become taut between adjacent PAAM–PAMPS contacts. In a simplistic view, we assume that the covalently cross-linked PAMPS network provides the anchoring points for the sliding PAAM chains; that is, the tube diameter is the average distance between adjacent junctions of the PAMPS network. In this view, L_c is considered as the contour length of a taut PAAM chain instead of a loose chain, and the value of t_c calculated with eq 2'' therefore represents an underestimation of the true value.

In the future, it will be desirable to relate the quantity τ_c to the quantity $(\chi_{1s} + \chi_{2s} - \chi_{12})$; more information at the atomic level is needed to establish a quantitative relation between these parameters. For the present time, we used viscosity data to estimate τ_c only because of its convenience and the lack of other alternatives. Therefore, the calculation given so far serves only to provide an order-of-magnitude estimation for τ_c . In this case, we find $\tau_c \approx 1.2 \times 10^{-19} \text{ N}$ per PAAM monomer unit.

An obvious shortfall of the deformation model depicted in Figure 1 is a clear violation of volume conservation in the process. During deformation, the total sample volume of the DN gel is likely to stay unchanged; that is, the sample deforms with a Poisson's ratio close to 0.5. This conservation of volume is also expected to be true for the PAMPS network, which is relatively rigid and brittle. The local swelling ratio in PAMPS network fragments is also likely to be the same as that of the sample before deformation. A direct consequence of the above statements is that the PAMPS network must occupy the entire sample volume during and after deformation. Even in deformed samples, the PAMPS network will be broken up to small pieces with a minimum dimension of $2t_c$; these pieces are expected to distribute and fill the entire sample volume. The broken PAMPS network fragments might serve as cross-links of the sliding type to reinforce the elastic modulus of the PAAM chains. Although a detailed volume-conservation model (for both sample volume and PAMPS volume) for DN gel deformation is yet to be proposed, it is possible that the primary deformation mode is shear rather than tensile as illustrated in Figure 1. Even for a shear-dominated process, the steps outlined in this work to estimate stress transfer between linear PAAM chains and the PAMPS network are still valid.

The breaking up of PAMPS network is expected to occur not only along the stretch direction as shown in Figure 1, but also in the perpendicular direction. The results shown in Figure 3 support this notion of PAMPS breakup, as the forward scattering intensity perpendicular to the stretch direction was more enhanced than that in the parallel direction. In addition, the increase in the forward scattering intensity from the PAMPS network persisted even after the deformation had relaxed and

the shape had been restored to its undeformed state. This result clearly indicates permanent damage in the structure of the PAMPS network upon deformation. This type of irreversibility in the forward scattering intensity is absent for the PAAm component as shown in Figure 2, where the intensity recovers almost completely to its value before deformation.

The calculated value of the periodicity for cracks at 1.16 μm raises an interesting issue about chain length as the contour length of a PAAm chain with molar mass of 10^6 is merely 2 μm . In this work, the molar mass of linear chains was considered to be infinite, and entanglements or unintentional cross-linking among PAAm chains must play an important role in the stress transfer. However, entanglements among high-molar-mass linear PAAm chains in solution by themselves are not sufficient to bring about the toughness observed in the PAMPS/PAAm DN gel. Regarding the toughening mechanism of this DN gel, we believe that the deformation-induced out-of-phase concentration fluctuations within the PAMPS and PAAm components constitute at least a portion of the energy dissipation process. The amount of dissipated energy is proportional to $\delta\phi(\chi_{1s} + \chi_{2s} - \chi_{12})$, where $\delta\phi$ represents the magnitude of the concentration fluctuations and its value can be determined from the SANS results in Figure 2. Work is ongoing to determine its magnitude and, hence, the possible significance of this process.

The only floating parameter in the deformation mechanism discussed above is c , the inverse fraction of load-bearing PAAm chains across an existing crack. Its value was set at unity, implying that every single PAAm chain carries the load. In the following discussion, the value of c is estimated from the tensile stress-strain results of Webber et al.²⁴ by applying rubber elasticity theory. More specifically, we use the shear modulus of DN gels at small strain after an initial large deformation (Figure 9 of ref 24) to estimate the number of active elastic chains per unit volume. Assuming that the relation $G = nRT$ holds for small biaxial deformations (compression), the elastic chain density can be calculated as 6 mol/m³ or 3.6×10^{-6} chains/Å³. This value translates into a volume of 2.8×10^5 Å³/chain and a cross-sectional area of 4.3×10^4 Å²/chain if one assumes that the PAMPS network fragments remain elastically rigid. These inputs return a value of 18.9 for c , which suggests that only about 5% of the PAAm chains are load-bearing. This value of c also revises our previous estimate of t_c to 1.26 μm , which is still of the same order of magnitude. Although we considered the effect of dilution while relating the stress to the elastic chain density, we did not consider the reinforcement effect from PAMPS fragments/blocks that are far more rigid than the elastic PAAm chains. Nevertheless, the above simple calculation suggests that letting c equal unity is not likely to result in an error in the order-of-magnitude estimation of t_c .

Conclusions

SANS analysis indicates that the deformation of DN gels results in out-of-phase concentration fluctuations between PAMPS and PAAm with a repeat spacing of ~ 1.5 μm and an irreversible change in PAMPS network structure. A stress-transfer mechanism between the PAMPS network and the linear PAAm chains is proposed as the underlying molecular mechanism for the formation of cracks with such a regular spacing. The monomer friction coefficient was estimated from the zero-shear viscosity data for PAMPS/PAAm solution blends at a composition similar to that of the DN gels. The combination of this friction coefficient and the critical shear rate in solution blend viscosity measurements yielded a value of 1.16 μm for the spacing between cracks, which is surprisingly close to that

observed in SANS measurements. Only a shear-rate-independent critical stress was considered in our model to calculate stress transfer between the linear PAAm chains and the PAMPS network; the resultant mechanical properties including toughness are thus independent of deformation rate. This is consistent with the experimental observation that the toughness of DN gels is almost independent of the deformation rate.

The deformation model introduced in this work serves to address only one of the necessary conditions for the formation of multiple cracks with a regular spacing in DN gels. The other necessary condition for multiple cracks to occur is the strain hardening of the PAAm chains, which is known to occur in semidilute aqueous PAAm solutions.⁴⁵ Strain hardening driven by intermolecular complexation via hydrogen bonding between two polymers was also recently shown to be a key feature in interpenetrating polymer network hydrogels.⁴⁶ A crack-opening mode in tension was the only deformation process considered in this model to highlight the importance of stress transfer between PAMPS and PAAm. Other important aspects of DN gel deformation such as the volume conservation of the whole sample and the PAMPS gel are not included. Work is ongoing to develop a stress-transfer model capable of addressing these deficiencies.

Acknowledgment. We thank Dr. John Barker and Dr. David Mildner for their support during USANS measurements. The neutron research facilities used in this work are supported by the National Institute of Standards and Technology, U.S. Department of Commerce. This work also utilized facilities supported in part by the National Science Foundation under Agreement No. DMR-0454672. J.P.G. acknowledges a Grant-in-Aid for Fundamental Research A and a Grant-in-Aid for Creative Scientific Research from the Ministry of Education, Science, Sports and Culture of Japan.

References and Notes

- (1) Haraguchi, K.; Takeshita, T. *Adv. Mater.* **2002**, *14*, 1121.
- (2) Okumura, Y.; Ito, K. *Adv. Mater.* **2001**, *13*, 485.
- (3) Karino, T.; Okumura, Y.; Zhao, C.; Kataoka, T.; Ito, K.; Shibayama, M. *Macromolecules* **2005**, *38*, 6161.
- (4) Okumura, Y. *Kobunshi Ronbunshu* **2005**, *62*, 380–389.
- (5) Zhao, C.; Domon, Y.; Okumura, Y.; Okabe, S.; Shibayama, M.; Ito, K. *J. Phys. Condens. Matter* **2005**, *17*, S2841.
- (6) Ito, K. *Polym. J.* **2007**, *39*, 489–499.
- (7) Fleury, G.; Schlatter, G.; Brochon, C.; Travelet, C.; Lapp, A.; Lindner, P.; Hadziioannou, G. *Macromolecules* **2007**, *40*, 535–543.
- (8) Karino, T.; Shibayama, M.; Ito, K. *Physica B* **2006**, *385*, 692–696.
- (9) Can, V.; Abdurrahmanoglu, S.; Okay, O. *Polymer* **2007**, *48*, 5016–5023.
- (10) Okay, O.; Oppermann, W. *Macromolecules* **2007**, *40*, 3378–3387.
- (11) Zhu, M. F.; Liu, Y.; Sun, B.; Zhang, W.; Liu, X. L.; Yu, H.; Zhang, Y.; Kuckling, D.; Adler, H. J. P. *Macromol. Rapid Commun.* **2006**, *27*, 1023–1028.
- (12) Xia, X. H.; Yih, J.; S'Souza, N. A.; Hu, Z. B. *Polymer* **2003**, *44*, 3389–3393.
- (13) Gong, J. P.; Katsuyama, Y.; Kurokawa, T.; Osada, Y. *Adv. Mater.* **2003**, *15*, 1155–8.
- (14) Nakayama, A.; Kakugo, A.; Gong, J. P.; Osada, Y.; Takai, M.; Erata, T.; Kawano, S. *Adv. Funct. Mater.* **2004**, *14*, 1124.
- (15) Yasuda, K.; Gong, J. P.; Katsuyama, Y.; Nakayama, A.; Tanabe, Y.; Kondo, E.; Ueno, M.; Osada, Y. *Biomaterials* **2005**, *26*, 4468.
- (16) Kaneko, D.; Tada, T.; Kurokawa, T.; Gong, J. P.; Osada, Y. *Adv. Mater.* **2005**, *17*, 535–538.
- (17) Tanaka, Y.; Osada, Y.; Gong, J. P. *Prog. Polym. Sci.* **2005**, *30*, 1–9.
- (18) Vendamme, R.; Onoue, S.-Y.; Nakao, A.; Kunitake, T. *Nat. Mater.* **2006**, *5*, 494–501.
- (19) Shull, K. R. *J. Polym. Sci. B: Polym. Phys.* **2006**, *44*, 3436–9.
- (20) Okamura, K. *Europhys. Lett.* **2004**, *67*, 470–6.
- (21) Tanaka, Y.; Kuwabara, R.; Na, Y.-H.; Kurokawa, T.; Gong, J. P.; Osada, Y. *J. Phys. Chem. B* **2005**, *109*, 11559–11562.

- (22) Huang, M.; Furukawa, H.; Tanaka, Y.; Nakajima, T.; Osada, Y.; Gong, J. P. *Macromolecules* **2007**, *40*, 6658–6664.
- (23) Brown, H. R. *Macromolecules* **2007**, *40*, 3815.
- (24) Webber, R. E.; Creton, C.; Brown, H. R.; Gong, J. P. *Macromolecules* **2007**, *40*, 2919.
- (25) Tominaga, T.; Tirumala, V. R.; Lee, S.; Lin, E. K.; Gong, J. P.; Wu, W. L. *J. Phys. Chem.* **2008**, *112*, 3903–3909.
- (26) Kelly, A.; Tyson, W. R. *J. Mech. Phys. Solids* **1965**, *13*, 329.
- (27) Certain equipment, instruments, or materials are identified in this article in order to adequately specify the experimental details. Such identification does not imply recommendation by the National Institute of Standards and Technology, nor does it imply the materials are necessarily the best available for the purpose.
- (28) Tominaga, T.; Tirumala, V. R.; Lin, E. K.; Gong, J. P.; Furukawa, H.; Osada, Y.; Wu, W.-L. *Polymer* **2007**, *48*, 7449–7454.
- (29) Flory, P. J. *Principles of Polymer Chemistry*; Cornell University Press: Ithaca, NY, 1953.
- (30) Glinka, C. J.; Barker, J. G.; Hammouda, B.; Krueger, S.; Moyer, J. J.; Orts, W. J. *J. Appl. Crystallogr.* **1998**, *31*, 430–445.
- (31) Barker, J. G.; Glinka, C. J.; Moyer, J. J.; Kim, M.-H.; Drews, A. R.; Agamalian, M. *J. Appl. Crystallogr.* **2005**, *38*, 1004.
- (32) Kline, S. R. *J. Appl. Crystallogr.* **2006**, *39*, 895.
- (33) The uncertainty in measured neutron scattering and viscosity data is less than the size of the markers used unless explicitly shown using error bars.
- (34) Bastide, J.; Leibler, L.; Prost, J. *Macromolecules* **1990**, *23*, 1821–1825.
- (35) Mendes, E.; Lindner, P.; Buzier, M.; Boue, F.; Bastide, J. *Phys. Rev. Lett.* **1991**, *66*, 1595–1598.
- (36) Karino, T.; Okumura, Y.; Zhao, C.; Kataoka, T.; Ito, K.; Shibayama, M. *Macromolecules* **2005**, *38*, 6161–6167.
- (37) Miyazaki, S.; Karino, T.; Endo, H.; Haraguchi, K.; Shibayama, M. *Macromolecules* **2006**, *39*, 8112–8120.
- (38) DiBenedetto, A. T. *Pure Appl. Chem.* **1985**, *57*, 1659.
- (39) Na, Y. H.; Tanaka, Y.; Kawauchi, Y.; Furukawa, H.; Sumiyoshi, T.; Gong, J. P.; Osada, Y. *Macromolecules* **2006**, *39*, 4641.
- (40) Kausch, H. H. *Phys. Solid State* **2005**, *47*, 906.
- (41) Bohdanecký, M.; Petrus, V.; Sedláček, B. *Makromol. Chem.* **1983**, *184*, 2061.
- (42) van Meerveld, J. *Rheol. Acta* **2004**, *43*, 615.
- (43) Kulicke, W. M.; Kniewske, R.; Klein, J. *Prog. Polym. Sci.* **1982**, *8*, 373.
- (44) Ferry, J. D. *Viscoelastic Properties of Polymers*, 3rd ed.; John Wiley & Sons: New York, 1980; p 510.
- (45) Schuberth, S.; Munstedt, H. *Rheol. Acta* **2008**, *47*, 139–147.
- (46) Myung, D.; Koh, W.; Ko, J.; Hu, Y.; Carraso, M.; Noolandi, J.; Ta, C. N.; Frank, C. W. *Polymer* **2007**, *48*, 5376–5387.

JP8002454